

## Inspection of Thin Copper Heat Exchanger Tubes Using SQUID-NDE System

Yoshimi Hatsukade<sup>1,a</sup>, Shinya Okuno<sup>1,b</sup>, Kazuaki Mori<sup>2,c</sup> and Saburo Tanaka<sup>1,d</sup>

<sup>1</sup>Department of Ecological Engineering, Toyohashi University of Technology,  
1-1 Hibarigaoka, Tenpaku-cho, Toyohashi, Aichi 441-8580, Japan

<sup>2</sup>Sumitomo Light Metal Industries, Ltd., Copper Works, 100 Ougishinmichi, Ichinomiya-cho,  
Hoi-gun, Aichi 441-1295, Japan

<sup>a</sup>hatukade@eco.tut.ac.jp, <sup>b</sup>ex043808@mail.eco.tut.ac.jp,  
<sup>c</sup>KAZUAKI\_MORI@mail.sumitomo-lm.co.jp, <sup>d</sup>tanakas@eco.tut.ac.jp

**Keywords:** SQUID, Copper Heat Exchanger Tube, Eddy Current, Micro Flaw

**Abstract.** This study is aimed at developing an eddy-current-based SQUID-NDE system for in-situ inspection of micro flaws on thin copper heat exchanger tubes. The system employs a high temperature superconductor (HTS-) SQUID gradiometer and a Helmholtz-coil-type inducer. As specimens, copper tubes 6.35 mm in outer diameter and 0.8 mm in thickness with artificial surface flaws of several tens  $\mu\text{m}$  in depth were inspected using the system. Magnetic response due to a flaw of 10  $\mu\text{m}$  in depth on the tube moving at 32 m/min was successfully detected while applying an excitation field of 10  $\mu\text{T}$  at 3 kHz to the tube. Numerical simulations were also conducted to evaluate how many sensors would be required for inspection around the circumference of an entire tube.

### Introduction

In recent years, the copper heat exchanger tubes used in, e.g., air conditionings, have a thickness of less than 1 mm in order to extract better performance [1]. During the making process of the tubes, flaws have accidentally occurred on the surfaces of the tubes. The flaws are lengthened and thinned during the process, then become very shallow. In the case of such thin tubes, even a micro flaw of only a few tens  $\mu\text{m}$  in depth will be a potential cause of a tube breakage, when the tubes would be bended or flared in post processes. For quality control in the tube factories, eddy current testing and ultrasonic testing have been employed to detect defects in the tubes during the making process [1-3]. However, it is difficult by the traditional NDE systems on the market to detect such shallow flaws of less than 50  $\mu\text{m}$  in depth. Thus, a more sensitive NDE technique is strongly demanded by manufacturers and users of the tubes.

Superconducting quantum interference devices using high temperature superconductors such as  $\text{YBa}_2\text{Cu}_3\text{O}_{7-x}$  (HTS-SQUIDs) are the uncontested magnetically sensitive sensors with the field resolution of a few tens  $\text{fT}/\text{Hz}^{1/2}$  from DC up to about 1 MHz [4]. Taking advantage of such high sensitivity in the wide frequency range, the field of SQUID-NDE has been widely explored since 1985. In the beginning, low temperature superconductor SQUIDs were used, and then replaced by HTS-SQUIDs in the 1990 up to date [5,6]. Especially for detection of defects, such as cracks, inclusions, or holes in variety of metallic materials and structures, eddy-current-based SQUID-NDE technique has been studied by many researchers [7-9]. This technique has some significant merits such as high field resolution, high spatial resolution, ability to detect deep-lying defects, and unnecessary of contact with objects under test.

We have studied the SQUID-NDE application for the inspection of micro flaws on the copper heat exchanger tubes. We have already showed that it is possible by the technique to detect a 10- $\mu\text{m}$ -depth flaw of 0.1 mm in width and 15 mm in length on slowly and stepwise moving tubes in our laboratory [10,11]. However, for practical use in tube factories, it is necessary for the SQUID-NDE technique to have robustness against environmental noises and correspondence to fast transfer of the tubes, since

the electromagnetic environment in the factories must be noisy and the tubes in the making process are transferred at high speed (more than 100 m/min).

To meet these requests, we have constructed an eddy-current-based SQUID-NDE system for in-situ inspection on the copper heat exchanger tubes. The system employs an HTS-SQUID gradiometer, which is expected to cancel the environmental magnetic noise, and an electric motor to move a tube continuously and fast. In this paper, the details of the system is described, and then detection of surface flaws of a few tens  $\mu\text{m}$  in depth on the copper tubes moving at up to 32 m/min were carried out to demonstrate the detection ability of the system.

### SQUID-NDE System for Copper Tubes

**Principle of SQUID-NDE technique on tubes.** In the making process of the copper heat exchanger tubes, flaws that occurred on the tubes are lengthened along the axis of the tube and thinned. To detect such long and shallow flaws, a Helmholtz-coil-type inducer composed of two field coils is suitable because it induces eddy current circulating around the circumference of a tube (perpendicular to the axis of the tube) when the tube passes through the inducer. Such eddy current efficiently flows across the flaw, and then is disturbed by the flaw. The disturbed eddy current generates an anomalous magnetic response due to the flaw around it. The schematic image of the SQUID-NDE technique on the copper heat exchanger tube with a flaw on its surface is illustrated in Fig. 1. A copper tube under test is moved through a Helmholtz-coil-type inducer, which applies an excitation field to the tube. An HTS-SQUID gradiometer, which is located in the middle of the inducer and above the tube, measures the anomalous magnetic signal generated by the disturbed eddy current.

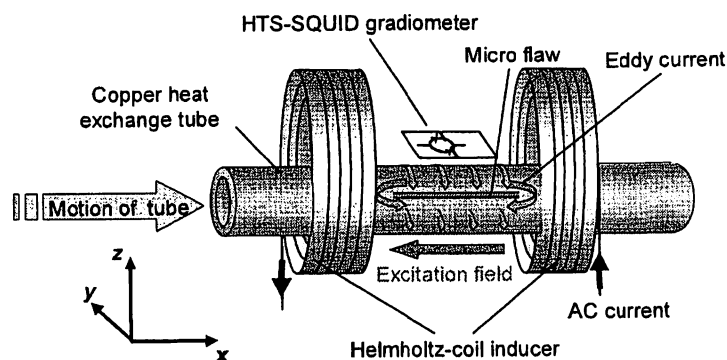


Fig. 1 Schematic image of the eddy-current-based SQUID-NDE technique on a copper tube.

**Details of SQUID-NDE System.** A SQUID-NDE system for copper heat exchanger tubes was constructed in an electromagnetically shielded room. The system is composed of an HTS-SQUID gradiometer with SQUID electronics, a portable FRP cryostat, a Helmholtz-coil-type inducer with  $xyz$  coil position adjustor, a current supplier, a lock-in amplifier, an electric motor and rail, and a PC. Fig. 2 (a) shows the schematic illustration of the system. The HTS-SQUID gradiometer is a direct-coupled type, and has differential rectangular pick-up coils. The size of single pick-up coil and the baseline length of the gradiometer are 2.88 mm x 3.6 mm and 3.6 mm, respectively. The details of the gradiometer is described elsewhere [11]. An FPR cryostat that can hold liquid nitrogen for 7 hours was used to cool the SQUID at around 77 K. The minimum standoff distance between the SQUID and the room temperature is about 0.5 mm, which is separated by a thin sapphire window. The Helmholtz-coil-type inducer was set in the polymeric  $xyz$  coil position adjustor, which is used to minimize the excitation magnetic flux coupled to the SQUID by adjusting the position of the inducer relative to the SQUID. This procedure is important for this kind of technique to keep the wide dynamic range of the SQUID. The SQUID was set between two field coils of the inducer. The turn number and dimensions of each field coil are 1000 and 50 mm in diameter and 45 mm in length,

respectively. The field coils were separated with a distance of 36 mm between both coil ends while aligning the centers of both coils. The electric motor can move a tube on the rail at up to 32 m/min. The magnetic flux noise of the system measured by means of a flux-locked loop operation is  $60 \mu\phi_0/\text{Hz}^{1/2}$  from 20 Hz to 5 kHz, where  $\phi_0 = 2.07 \times 10^{-15}$  Wb is the magnetic flux quantum. Corresponding field gradient is  $6 \text{ pT/cm/Hz}^{1/2}$ . The system noise spectrum is shown in Fig. 2 (b).

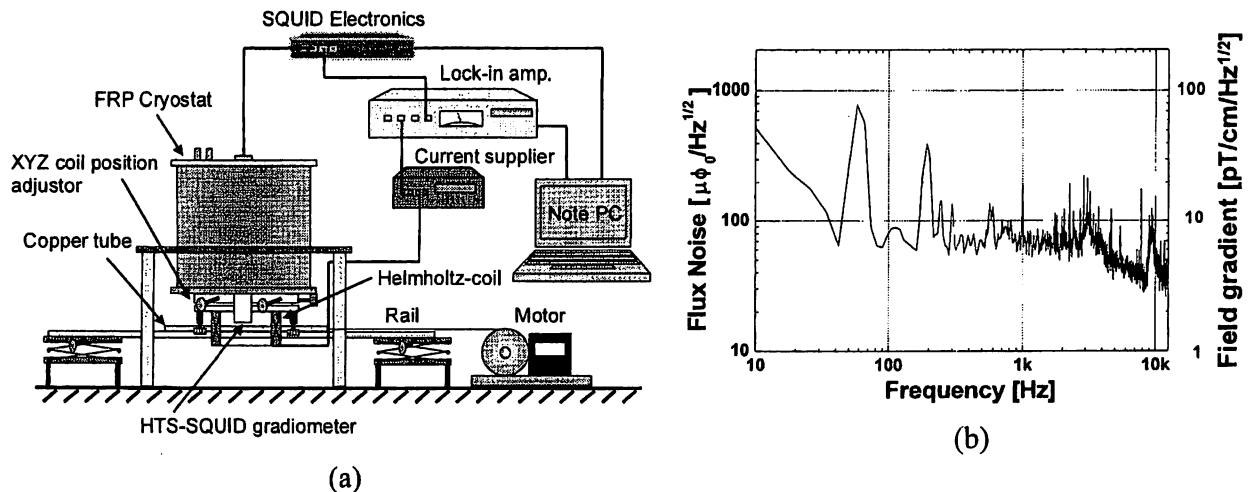


Fig. 2 SQUID-NDE prototype system for a moving copper tube. (a) Schematic system diagram. (b) System noise spectrum.

**Specimens.** Copper heat exchanger tubes that had artificial shallow flaws with various depths on surfaces were prepared as specimens. These tubes were selected from commercial products. The dimensions of all the tubes are 6.35 mm in outer diameter, 0.8 mm in thickness and 300 mm in length. The dimensions of the flaws are 100  $\mu\text{m}$  in width and 15 mm in length and the depths of the flaws are 100  $\mu\text{m}$ , 50  $\mu\text{m}$ , and 30  $\mu\text{m}$ , respectively. A shallowest flaw of 10  $\mu\text{m}$  in depth, 100  $\mu\text{m}$  in width and 25 mm in length was also made. The flaws were made using an electric discharge machine. Fig. 3 shows a specimen with a micro flaw on the surface.

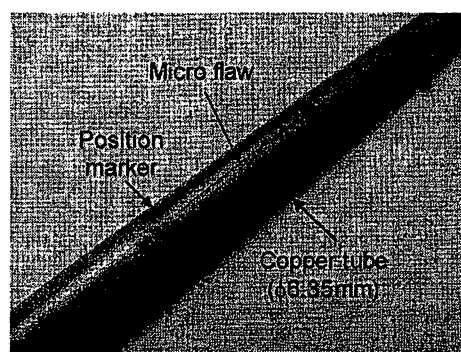


Fig. 3 Tube specimen with a micro flaw.

### Measurements and Results

**Measurements.** We evaluated the detection ability of the SQUID-NDE system by inspecting the flaws on the tube specimens. A sinusoidal current of 3 kHz was supplied to the Helmholtz-coil-type inducer to apply an excitation field to the specimen. The magnetic flux density  $B_x$  (parallel to the axis of the tube) at the middle of the two field coils was about 10  $\mu\text{T}$  (See Fig. 1). The tube specimens were moved through the inducer at the velocity of 1.6 – 32 m/min. The flaws were set to be located on the

top of the tube with a distance of 1.5 mm between the HTS-SQUID gradiometer and the top of the tube. The HTS-SQUID gradiometer was set to measure the field gradient in the  $x$ -direction of the vertical magnetic flux density,  $dB_z/dx$ . The SQUID output was recorded in the PC with the sampling frequency of 100 – 1000 Hz according to the tube velocity. The position of the inducer was carefully adjusted before the measurements to minimize the SQUID output due to the excitation field itself.

**Results.** The experimental results on the tube specimens with 50- $\mu\text{m}$ -, 30- $\mu\text{m}$ -, and 10- $\mu\text{m}$ -depth flaws using the excitation field of 10  $\mu\text{T}$  at 3 kHz are shown in Fig. 4 (a) – (c), respectively. The tubes were moved at 1.6 m/min. In each figure, a schematic view of the flawed tube specimen is depicted together for reference of the position of the flaw. Anomalous magnetic responses due to the micro flaws are observed above and around the flaws. Even the 10- $\mu\text{m}$ -depth flaw was successfully detected. The peak-peak amplitudes due to the flaws are approximately proportional to the flaw depth. Fig. 4 (d) shows the result on the 10- $\mu\text{m}$ -depth flaw on the tube moving at 32 m/min. Almost the same waveform as Fig. 4 (c) was measured. The noise in Fig. 4 (d) is somewhat smaller than Fig. 4 (c) (indicated by the circles) although the moving speed was faster. That's may be due to a bit larger vibration of the specimen caused by the friction between the rail and the specimen when the specimen was moved slowly. The improvement on the system that suppresses the tube vibration less than 10 - 20  $\mu\text{m}$  should be required for practical use.

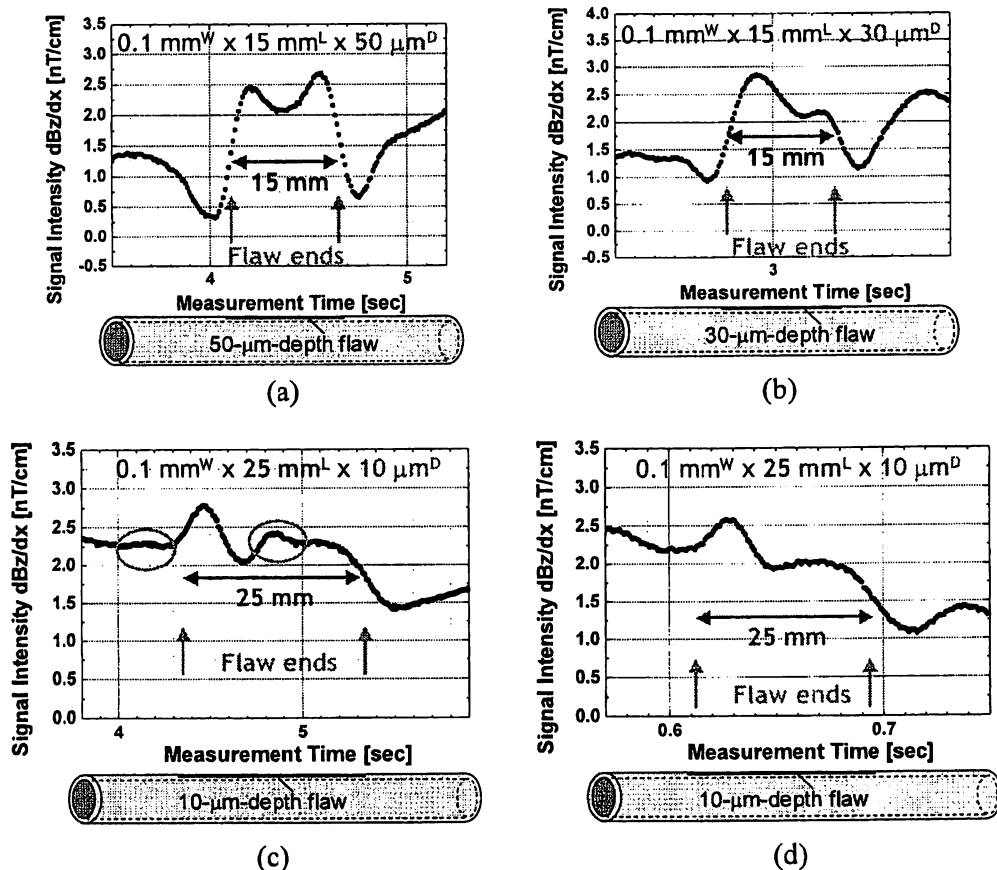


Fig. 4. Waveforms obtained by the measurements on (a) 50- $\mu\text{m}$ -depth flaw, (b) 30- $\mu\text{m}$ -depth flaw, (c) 10- $\mu\text{m}$ -depth flaw and (d) 10- $\mu\text{m}$ -depth flaw. In the measurement on (d), the specimen was moved at 32 m/min, while in the other cases (a) – (c), they were moved at 1.6 m/min.

### Simulation

As for the above-mentioned experiments, all flaws were located on the top of the tube where was closest to the SQUID. However, in the real situations, flaws do not always locate there. Thus, we

evaluated how the magnetic signal due to a flaw would change in the cases that the flaws did not locate at the top of a tube by numerical simulation. Fig. 5 shows the simulation model that we employed. The left-hand drawing in the figure shows the cross-sectional image of a tube with a flaw. In this simulation, we assumed that the magnetic field generated by an eddy current disturbed due to a flaw could be approximated by a magnetic field generated by virtual current dipoles on the flaw position. As shown in the figure, a current dipole has a current moment  $Q$ . We defined the angle  $\theta$  is the angle from the  $xz$ -plane to the flaw in the  $yz$ -plane. The magnetic field  $B(r)$  due to the virtual dipoles at the measurement point  $r$  was calculated using the following equation,

$$B(r) = \frac{\mu_0}{4\pi} \sum_i \frac{Q \times (r - r_i)}{|r - r_i|^3} \quad (1)$$

where  $\mu_0$  is the permeability of the air, and  $r_i$  is the vector toward a current dipole while  $i$  is the index number of a current dipole. The right-hand drawing in Fig. 5 shows the top view of the tube specimen. The dimensions of a tube specimen were assumed to be same as the tubes used in the experiments. The dimensions of the flaw were 15 mm in length, 0.1 mm in width, and 0.5 mm in depth. We assumed that the aligned virtual current dipoles on the flaw position were composed of 16 dipoles with separation of 1 mm to each other for simplicity. The current moment of a dipole  $Q$  was assumed to have amplitude of 240 nAm. The height of the measurement points from the top of the tube was 1.825 mm. We calculated the field gradient  $dB_z/dx$  generated by the aligned current dipoles at the measurement points as shown in Fig. 5, while changing  $\theta$  stepwise with a step of 15 degrees.

Fig. 6 (a) shows the simulation results, which give the amplitudes of field gradient as a function of the measurement point on the  $x$ -axis with various  $\theta$ . The simulation waveforms approximately resembles to those shown in Fig. 4. The signal amplitude decreases rapidly with the increase of angle  $\theta$ . The amplitude is null at  $\theta = 90$  degrees, because the virtual current dipole completely oriented toward the  $z$ -direction and such dipoles generate no magnetic component toward  $z$ -direction. Fig. 5 (b) shows the plot of the peak-peak amplitude due to the dipoles versus the angle  $\theta$ . The peak-peak amplitudes are normalized by the amplitude at  $\theta = 0$ . If the threshold would be determined to be 20 % of the peak-peak amplitude at  $\theta = 0$ , the plot indicates one sensor can cover the angle about 90 degrees. It leads to that at least four sensors should be necessary for inspection around a circumference of an entire tube in the case that the tube cannot be rotated, as in the factory.

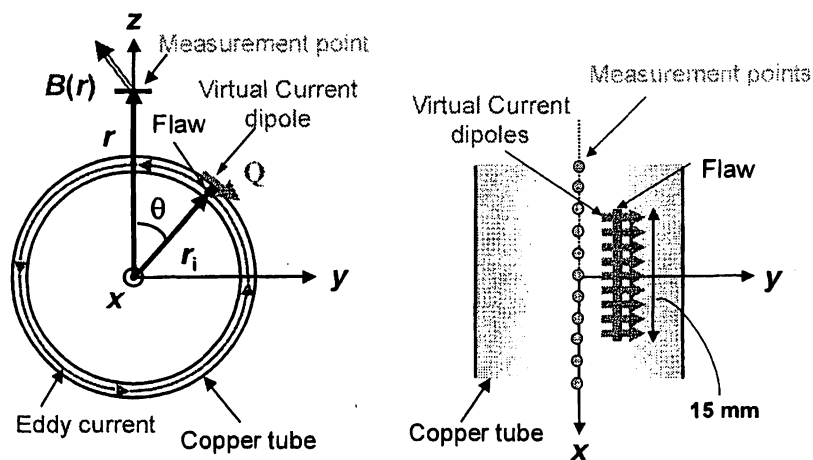


Fig. 5 Simulation model of a copper tube with a flaw while an eddy current is induced in the tube, which is repalced by virtual current dipoles. Left-hand figure: Cross-sectional view. Right-hand.

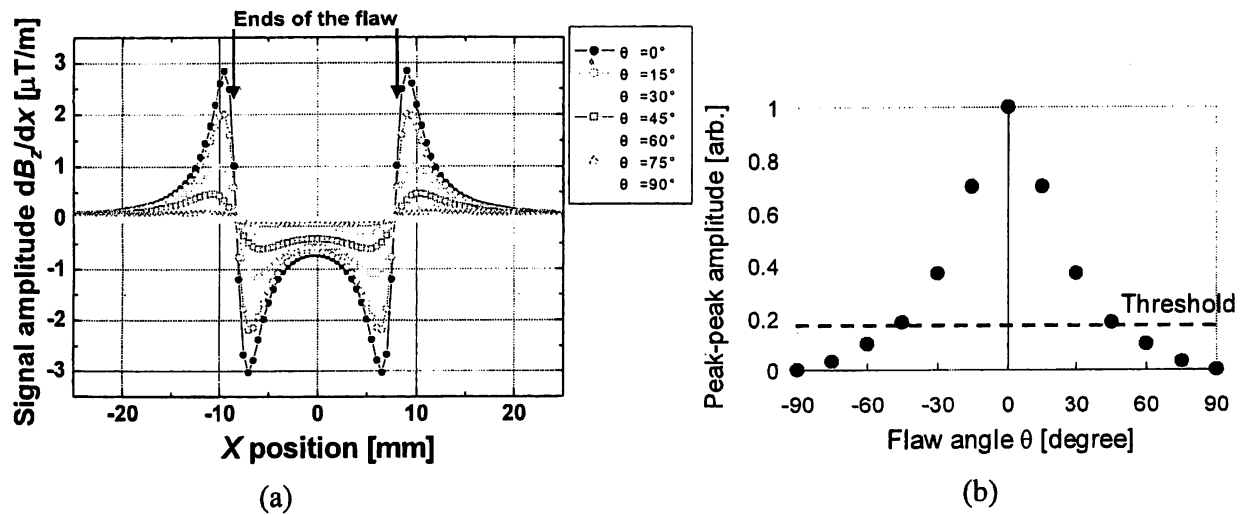


Fig. 6 The simulation results. (a) Waveforms due to the current dipoles while changing the  $\theta$  from 0 to 90 degrees. (b) Normalized peak-peak amplitude vs. flaw angle  $\theta$ .

### Summary

An eddy-current-based SQUID-NDE system has been developed for in-situ inspection of thin copper heat exchanger tubes. With an excitation field of  $10 \mu\text{T}$  at 3 kHz, the SQUID-NDE system successfully detected a magnetic field gradient signal due to the  $10\text{-}\mu\text{m}$ -depth flaw on the tube, which was moved at 32 m/min under the HTS-SQUID gradiometer. Numerical simulations were also conducted. The simulation results suggest at least 4 sensors may be required for inspection around the circumference of an entire tube.

### References

- [1] For example, SUMITOMO Light Metal Industries, LTD., <http://www.sumitomo-lm.co.jp>.
- [2] A.J. Trivedi and R.R. Parikh: Proc. 14<sup>th</sup> World Conf. Non-Destructive Testing, Vol. 3 (1996), p.1729.
- [3] H.H. Roasmussen, H. Kristensen and L. Jeppesen: 7<sup>th</sup> European Conference On Non-Destructive Testing, Vol. 3 (1996), p. 739.
- [4] A. Barone: *Principles and Applications of Superconducting Quantum Interference Device* (World Science, 1992).
- [5] W.N. Podney: IEEE Trans. Appl. Supercond., Vol. 3 (1993), p. 1914.
- [6] A. Ruosi, M. Valentino, G. Peluso and G. Pepe: IEEE Trans. Appl. Supercond., Vol. 11 (2001), p. 1172.
- [7] A. Cochran, G. B. Donaldson, L. N. C. Morgan, R. M. Bowman and K. J. Kirk: Br. J. of NDT, Vol. 35 (1993), p. 173.
- [8] R. Hohmann, M. Maus, D. Lomparski, M. Greuneklee, Y. Zhang, H. -J. Krause, H. Bousack and A. I. Braginski: IEEE Trans. Appl. Supercond., Vol. 9 (1999), p. 3801.
- [9] Y. Hatsukade, M. S. Aly-Hassan, N. Kasai, H. Takashima, H. Hatta and A. Ishiyama: IEEE Trans. Appl. Supercond., Vol. 13 (2003), p. 207.
- [10] Y. Hatsukade, A. Kosugi, K. Mori and S. Tanaka, Jpn. J. Appl. Phys., Vol. 43 (2004), p. L1488.
- [11] Y. Hatsukade, A. Kosugi, K. Mori and S. Tanaka, Physica C, Vol. 426-431 (2005), p. 1585.